Compressibility and heat capacity of rotating plasma

V. I. Geyko and N. J. Fisch
Department of Astrophysical Sciences, Princeton University, Princeton, New Jersey 08544, USA

(Received 27 October 2016; accepted 23 January 2017; published online 9 February 2017)

A rotating plasma column is shown to exhibit unusual heat capacity effects under compression. For near equilibrium thermodynamics and smooth wall conditions, the heat capacity depends on the plasma density, on the speed of the rotation, and on the mass ratio. For a certain range of parameters, the storage of energy in the electric field produces a significant increase in the heat capacity. *Published by AIP Publishing.* [http://dx.doi.org/10.1063/1.4975651]

I. INTRODUCTION

The compression of rotating plasmas is of significant scientific interest, particularly in astrophysical applications, such as accretion disks.[1] To some extent, laboratory experiments[2,3] or numerical simulations as well[4,5] can exhibit the physics of the naturally occurring plasma. Ablation flows from a cylindrical wire array z-pinch, or laser generated jets,[6] can introduce angular flows through axial currents crossed with radial magnetic fields. As the ablated flows are then compressed radially, the plasma spins faster until centrifugal forces balance the pressure of the incoming radial flow. A supersonically spinning hollow ring plasma was obtained, with ion temperature $T_i \sim 60\,\mathrm{eV}$, electron temperature of $ZT_e \sim 200\,\mathrm{eV}$, and plasma density $10^{19}\,\mathrm{cm}^{-3}$.[3] A focus of previous studies of rotating and compressing plasma has been the transient dynamics of the rotating convergent flow, such as the formation of standing shocks.

In contrast, our interest here is in the equation of state of rotating plasma under compression, with particular interest in the compressibility and the heat capacity. We expect to find that the compressibility and heat capacity of the plasma depend on parameters such as the spinning velocity and the charge density. This will generalize the problem of compressibility of the spinning neutral gas, which exhibits a number of unusual features including a *rotation-dependent heat capacity*.[7]

The rotation-dependent heat capacity effect arises in neutral gas because, under an axial compression, a spinning gas becomes hotter and thus more uniformly distributed radially. Since the moment of inertia decreases, it must spin faster to conserve the angular momentum. That means that part of the energy of compression goes, not into heating the gas, but to making it spin faster. In other words, the bulk rotation comprises an extra degree of freedom for energy storage, thereby adding to the heat capacity, and curiously, making a spinning gas easier to compress axially than a non-spinning gas at the same temperature.

We can anticipate a similar effect for the spinning plasma; however, the heat capacity in plasma is more complicated. In plasma, there is also an electrostatic energy, which is coupled to the spinning velocity and similarly changes under compression. The question that we pose and answer here is how this electrostatic energy contributes to the plasma heat capacity.

The paper is organized as follows: In Sec. II, we write the basic equations of spinning plasma. In Sec. III, we derive the heat capacity and compression functions. In Sec. IV, we point out some features of the numerical techniques used in solving the basic equations. In Sec. V, we discuss our results and point out areas for future research.

II. BASIC EQUATIONS

Consider a cylindrical column of plasma with radius r_0 and length L rotating along $\hat{z}$ axis. The plasma cylinder is assumed to be long compared to its radius $L \gg r_0$, so that edge effects can be neglected, and the problem can be treated in 2D cylindrical geometry. In thermodynamical equilibrium, all sheared flows dissipate; hence, the solid body rotation is established with an angular velocity ω and temperature T. For simplicity, consider only a two-species plasma: electrons with charge $-q$ and mass m_e and ions with charge q and mass m_i. In principle, such an approach could be generalized to multi-ionized plasma or several species of ions with different masses and charges; however, two species are enough to capture the basic effects that will be important for heat capacity. Assume that the plasma is confined by *ideal* walls with free slip boundary conditions and perfectly insulating with respect to transport of heat or charge. Under rotation, we expect a radial electric field as the ions separate from electrons. In general, there could be an axial magnetic field, either imposed or as a result of azimuthally rotating charge.

The force balance equations in the radial direction, where pressure is balanced against the centrifugal force and the electro-magnetic force, then gives the following system of equations:

$$-m_e\omega^2 r n_e = -T\frac{\partial n_e}{\partial r} - n_e qE - n_e qB\frac{\omega r}{c}, \tag{1}$$

$$-m_i\omega^2 r n_i = -T\frac{\partial n_i}{\partial r} + n_i qE + n_i qB\frac{\omega r}{c}, \tag{2}$$

where n_e and n_i denote the electron and ion densities, respectively, E is the radial electric field, B is the axial magnetic field, and c is the speed of light.

To complete Eqs. (1) and (2), we write down the Maxwell's equations in cylindrical coordinates, assuming that the electric field has $\hat{r}$ and magnetic field has $\hat{z}$ components only

$$\frac{\partial(rE)}{\partial r} = 4\pi q r(n_i - n_e), \tag{3}$$

$$\frac{\partial B}{\partial r} = 4\pi \frac{\omega r}{c} q(n_i - n_e). \tag{4}$$

In the following, we will specialize the case where there is no externally imposed axial magnetic field. We will also specialize the case of non-relativistic rotation $\omega r_0 \ll c$, so that the internally generated axial magnetic field can be neglected since it goes like $\omega r_0/c$ in Eq. (4). Thus, we now consider the limit of non-magnetized plasma, where the magnetic field terms in Eqs. (1) and (2) vanish.

Hence, for the non-magnetized plasma, we now introduce dimensionless parameters, and rewrite Eqs. (1)–(3) in the compact form

$$-2\varphi_e x\tilde{n}_e = -\frac{\partial \tilde{n}_e}{\partial x} - 2\tilde{n}_e Q\tilde{E}, \tag{5}$$

$$-2\varphi_i x\tilde{n}_i = -\frac{\partial \tilde{n}_i}{\partial x} + 2\tilde{n}_i Q\tilde{E}, \tag{6}$$

$$\frac{\partial(x\tilde{E})}{\partial x} = x(\tilde{n}_i - \tilde{n}_e). \tag{7}$$

Here, the dimensionless parameters are the following:

$$N = \pi r_0^2 \bar{n} L, \quad \tilde{n}_{i,e} = \frac{n_{i,e}}{\bar{n}}, \quad r = x r_0,$$
$$E = 4\pi q \bar{n} r_0 \tilde{E}, \quad \varphi_{i,e} = \frac{m_{i,e}\omega^2 r_0^2}{2T},$$
$$Q = \frac{m_e \omega_{pe}^2 r_0^2}{2T} = \frac{2q^2 N}{LT}, \tag{8}$$

where N is the total number of electrons or ions.

This system in determined by 3 dimensionless parameters: φ_i, φ_e, and Q. The first two *spinning parameters* φ_i and φ_e have the same meaning as for the neutral gas case, i.e., the ratio of the rotation velocity at the periphery to the temperature, or in other words how strong the rotation is compared to the thermal energy. The new parameter, Q, shows the strength of electrostatic interaction. However, this term cannot be interpreted simply as a ratio of the total electrostatic energy to the temperature; rather it can be interpreted as the ratio of electrostatic energy to the temperature, if particle spatial distribution did not feel any electrostatic force. This interpretation will become clearer when we show the solution to these equations.

Equations (5)–(7) describe the equilibrium distribution of electrons and ions. While no fully analytical solution is possible, some analytical progress can be made by introducing the electric potential $\partial\Phi/\partial x = -E$. Both Eqs. (5) and (6) can then be integrated once to obtain

$$n_{e,i} = \bar{n}_{e,i} \exp(\varphi_{e,i} x^2 \pm 2Q\Phi) \tag{9}$$

which is exactly the Boltzmann distribution in a given potential.[8] The constants of integration, $\bar{n}_{e,i}$ are determined from the total particle conservation, namely

$$\int_0^1 2n_{i,e}(x) x dx = 1. \tag{10}$$

We can now solve for the potential using Poisson's equation, with charge density determined by Eq. (9)

$$(x\Phi')' = -x(\bar{n}_i e^{(\varphi_i x^2 - 2Q\Phi)} - \bar{n}_e e^{(\varphi_e x^2 + 2Q\Phi)}), \tag{11}$$

where the prime denotes a derivative with respect to x. The boundary conditions for Eq. (11) are

$$\Phi'(x=0) = \Phi'(x=1) = 0 \tag{12}$$

due to the total charge neutrality and Eq. (10) for normalization of $\bar{n}_{e,i}$. The density normalization in Eq. (10) also determines the arbitrary constant for the potential Φ.

Equation (11) can be solved numerically in given parameters, φ_i, φ_i, and Q. An example of such a solution is shown in Fig. 1. As the electrostatic interaction increases, the particle spatial distributions become closer and closer to each other. This occurs because, a larger separation will cause larger charge densities, hence larger fields. One can expect that for very large parameter Q we should have quasi neutrality and Debye screening.[9] Indeed, in Fig. 1 we can see a similar behavior for $Q = 200$: electron and ion distributions are nearly identical except for the boundary layer where electrons screen a little excessive space charge.

III. HEAT CAPACITY AND COMPRESSION FUNCTIONS

Generalizing the method employed in the case of neutral gas,[7] we now calculate how heat capacity changes in the presence of space charge. We will consider the modified heat capacity at a constant volume $\tilde{c}_v$. For non-spinning gas with no electrostatic interaction, one has the standard heat capacity coefficient $c_v = 1.5$ for mono atomic or $c_v = 2.5$ for diatomic gas. For spinning ideal gas, the heat capacity changes;[7] however, for spinning charged particles of different masses, there

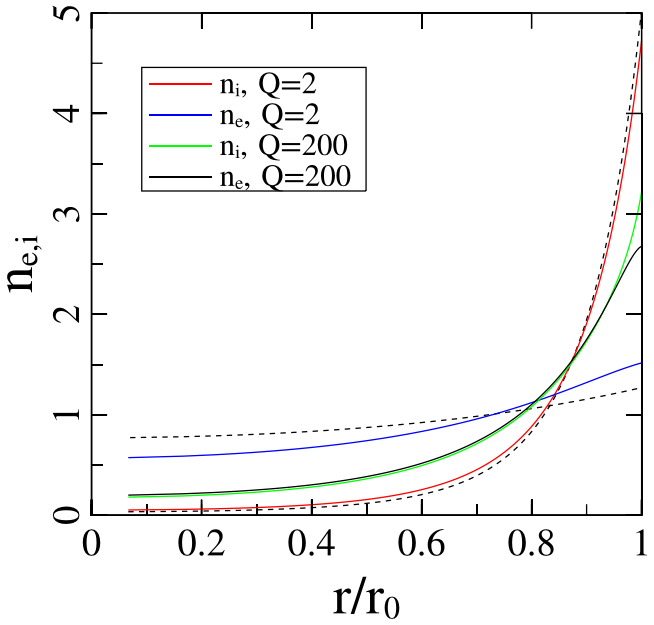

FIG. 1. Example of equilibrium density distribution for ions and electrons. Spinning parameters are fixed: $\varphi_i = 5$, $\varphi_e = 0.5$. Dashed black lines: ion and electron densities for $Q = 0$; red: ions for $Q = 2$; blue: electrons for $Q = 2$; green: ions for $Q = 200$; solid black: electrons for $Q = 200$.

is the additional effect of charge separation. The charge separation produces an electric field, and the stored energy in that field should affect the heat capacity.

Consider how the adiabatic compression is modified in the presence of spatial charge. Let us define a *compression function* c_f as the coefficient in the ODE

$$\frac{dV}{V} + c_f \frac{dT}{T} = 0. \tag{13}$$

For an axial compression, we will call $c_f = B$ and for radial compression $c_f = C$. In the case of ideal non-spinning gas $B = C = c_f = c_v$.

In order to find $\tilde{c}_v$, B, and C, we make use of the conservation of total angular momentum. We assume that heating or compression occurs on the time scale shorter than angular momentum dissipation, so that, for zero external magnetic field, the total angular momentum reads as

$$M = L\int_0^{r_0} 2\pi r dr \omega r^2 (n_e m_e + n_i m_i)$$
$$= \frac{2NT}{\omega}\int_0^1 2dx x^3 (\varphi_i \tilde{n}_i + \varphi_e \tilde{n}_e). \tag{14}$$

In order to calculate the total energy, we need to take into account also the electrostatic energy

$$W_E = \frac{L}{8\pi}\int_0^{r_0} 2\pi r dr E^2 = NTQ\int_0^1 2dx x \tilde{E}^2. \tag{15}$$

The total internal energy of the gas has three terms: thermal, rotational, and electrostatic.

$$U = (c_{vi} + c_{ve})NT + \frac{M\omega}{2} + W_E. \tag{16}$$

We now make use of the angular momentum conservation to find the relation between ω, T, L, and r_0

$$\frac{\partial M}{\partial L} dL + \frac{\partial M}{\partial r_0} dr_0 + \frac{\partial M}{\partial T} dT + \frac{\partial M}{\partial \omega} d\omega = 0. \tag{17}$$

For electrons and ions, the thermal contributions to the heat capacity can be taken to be equal, namely, $c_{ve} = c_{vi} = c_v$, which is equivalent to saying that the electrons and ions have no internal energy, only kinetic energy.

A. Heat capacity

The heat capacity at a constant volume per single particle is given by

$$\tilde{c}_v = \frac{1}{2N}\frac{dU}{dT} = c_v + \frac{M}{4N}\frac{d\omega}{dT} + \frac{1}{2N}\frac{dW_E}{dT}. \tag{18}$$

For the full derivative of electrostatic energy, we have

$$\frac{dW_E}{dT} = \frac{\partial W_E}{\partial T} + \frac{\partial W_E}{\partial \omega}\frac{d\omega}{dT} \tag{19}$$

and for $d\omega/dT$ we use Eq. (17), so the modified heat capacity reads as

$$\tilde{c}_v = c_v + \frac{1}{2N}\left(\frac{\partial W_E}{\partial T} - \frac{\partial M}{\partial T}\left(\frac{M}{2} + \frac{\partial W_E}{\partial \omega}\right)\left(\frac{\partial M}{\partial \omega}\right)^{-1}\right). \tag{20}$$

Partial derivatives here are taken numerically, as a difference of functions calculated on two close equilibria over the small change of the argument. Notice that the result of calculation does not depend on the form how we represent the function. For example, when we calculate the partial derivative of angular momentum M with respect to T we can use any of the forms in Eq. (14) (in the first case we have the contribution from integral only, in the second case from $\varphi_{i,e}$ and $2NT/\omega$ also) but the final value of the derivative is the same.

We are interested in correction to the standard coefficient c_v, and this correction, as we can see, has two parts. One is due to the change of rotational energy, and the other is due to the change in the electrostatic energy.

Figure 2 shows how the heat capacity modification $\tilde{c}_v - c_v$ depends on the spinning parameter for different values of the electrostatic interaction parameter Q. For $Q = 0$, we simply have a mixture of two types of neutral gases (black solid line): first the heat capacity grows from 0 to approximately 1/2 as the heavy rotating ions start to contribute to it; then it slowly grows to a saturation point approximately equal to 1, as the light electrons start spinning faster and faster. If we increase the electrostatic interaction, the heat capacity reaches the saturation point faster. This might be explained as follows: heavy ions attract electrons and pull them close, making the electron density distribution function nearly identical to the ion distribution function (as it is shown in Fig. 1 in case of $Q = 200$). As a result, the electrons would contribute more to the heat capacity.

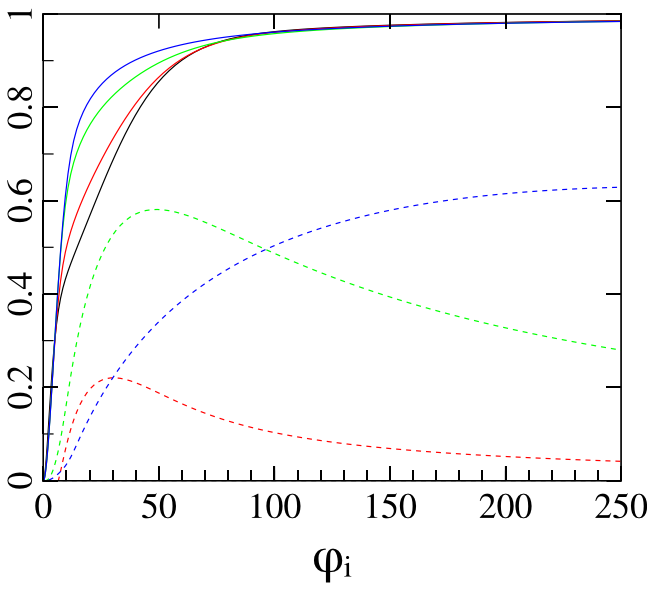

FIG. 2. Heat capacity correction and electrostatic contribution. Solid: $\tilde{c}_v - c_v$ vs. ion spinning parameter φ_i at a fixed ion-electron mass ratio $m_i/m_e = 10$. Dashed: electrostatic contribution (depicted on 5 times greater scale for better visibility). Black: $Q = 0$; red: $Q = 4.5$; green: $Q = 40.5$, blue: $Q = 364.5$.

However, the effect is not entirely due to spatial electron density re-distribution. We also plotted the total electrostatic term in modified heat capacity, which is

$$-\frac{1}{2N}\left(\frac{\partial W_E}{\partial T}-\frac{\partial M}{\partial T}\frac{\partial W_E}{\partial \omega}\left(\frac{\partial M}{\partial \omega}\right)^{-1}\right). \tag{21}$$

Note that its contribution is quite considerable. That means that, while the electrostatic contribution increases with increasing Q, the rotational contribution simultaneously decreases, so that the sum reaches saturation. Therefore, we cannot simply split the total contribution to the two parts and treat them somehow separately, but instead we need to consider the coupled contributions. In other words, we must also account for the fact that the electrons pull the ions back, thereby not letting them contribute as much to the heat capacity.

An interesting question is the heat capacity dependence on the mass ratio. Before, we had a fixed mass ratio $m_i/m_e = 10$, which was picked in order to demonstrate a clear saturation behavior as $\varphi_i \to \infty$. Intuitively, we understand that if the ion contribution saturates at $\varphi_i \sim 10$, the electron contribution should saturate at $\varphi_e \sim 10 m_i/m_e$. Therefore for a mass ratio of 10, we can capture this effect. But we are free to try different values, for example, $m_i/m_e = 100$. Fig. 3 demonstrates the same asymptotic behavior in φ_i as Fig. 2, but for $m_i/m_e = 100$, and electrostatic contribution depicted in the figure on 2 times greater scale. As we see, the electron contribution takes longer to catch up, and the electrostatic component is considerably bigger. However, the saturation behavior as $Q \to \infty$ and $\varphi \to \infty$ is approximately the same, so the total heat capacity correction does not exceed 1.

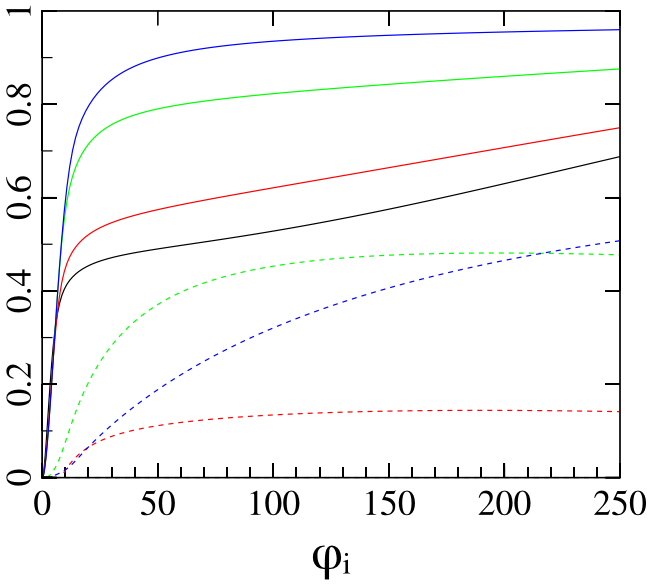

FIG. 3. Heat capacity correction and electrostatic contribution. Solid: $\tilde{c}_v - c_v$ vs. ion spinning parameter φ_i at fixed ion-electron mass ratio $m_i/m_e = 100$. Dashed: electrostatic contribution (depicted on 2 times greater scale for better visibility). Black: $Q = 0$; red: $Q = 4.5$; green: $Q = 40.5$, blue: $Q = 364.5$.

B. Axial compression

To derive the compression function for longitudinal adiabatic compression, we need to include all partial derivatives with respect to L and make use of the energy conservation $pdV + dU = 0$

$$-pdV = -2NT\frac{dL}{L} = 2c_v N dT + \frac{M}{2}d\omega + \frac{\partial W_E}{\partial L}dL + \frac{\partial W_E}{\partial T}dT + \frac{\partial W_E}{\partial \omega}d\omega. \tag{22}$$

Plug in $d\omega$ from Eq. (17) into Eq. (22) and combine all terms before dL and dT. Skipping simple algebra, obtain

$$B = \left(\frac{T}{L}\right)\frac{2c_v N + \frac{\partial W_E}{\partial T} - \frac{\partial M}{\partial T}\left(\frac{M}{2}+\frac{\partial W_E}{\partial \omega}\right)\left(\frac{\partial M}{\partial \omega}\right)^{-1}}{\frac{2NT}{L} + \frac{\partial W_E}{\partial L} - \frac{\partial M}{\partial L}\left(\frac{M}{2}+\frac{\partial W_E}{\partial \omega}\right)\left(\frac{\partial M}{\partial \omega}\right)^{-1}}. \tag{23}$$

Note that the behavior of the modified heat capacity looks similar to the axial compression function. In the case of neutral gas, there is no electrostatic energy, so the angular momentum does not depend on L. Thus, these two functions are identical, so that one can interchangeably use the terms compression function and heat capacity.[10] However, here we should distinguish these two. Note also that, as the mass ratio increases, we need considerably larger spinning parameters to reach saturation. Indeed, since we plot our variables as a function of ion spinning parameter, for large mass ratio, the electrons feel the spinning less, thus requiring the larger spinning parameter to reach saturation (Fig. 4).

C. Radial compression

For a radial compression, we take the same approach that we used for an axial compression. The main difference is in the pdV work that is given by $pdV = 2NT(\tilde{n}_e + \tilde{n}_i)\frac{dr_0}{r_0}$,

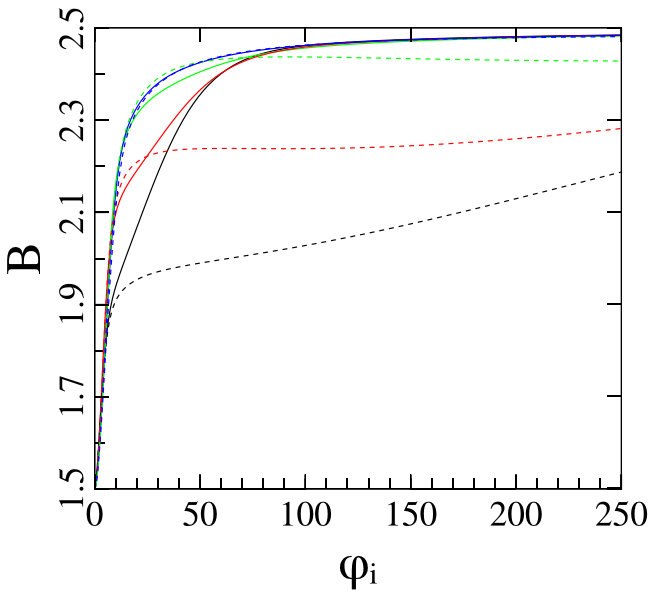

FIG. 4. Axial compression function for $c_v = 1.5$. Solid: $m_i/m_e = 10$; dashed: $m_i/m_e = 100$. Black: $Q = 0$; red: $Q = 4.5$; green: $Q = 40.5$, blue: $Q = 364.5$.

where densities are calculated at $r = r_0$. Following the same derivation that we used for longitudinal compression $\frac{dr_0}{r_0} + \frac{dT}{T}C$, obtain

$$C = \frac{2c_v N + \frac{\partial W_E}{\partial T} - \frac{\partial M}{\partial T}\left(\frac{M}{2} + \frac{\partial W_E}{\partial \omega}\right)\left(\frac{\partial M}{\partial \omega}\right)^{-1}}{\frac{2NT}{r_0}(\tilde{n}_e + \tilde{n}_i) + \frac{\partial W_E}{\partial r_0} - \frac{\partial M}{\partial r_0}\left(\frac{M}{2} + \frac{\partial W_E}{\partial \omega}\right)\left(\frac{\partial M}{\partial \omega}\right)^{-1}}. \tag{24}$$

The densities in the first term in the denominator are taken at $x = 1$. In Fig. 5, we can see C as a function of the ion spinning parameter for mass ratios $m_i/m_e = 10$ and $m_i/m_e = 100$. The behavior is apparently quite complicated and is sensitive to both the parameter Q and the mass ratio. Moreover, it is no longer monotonic in φ_i, but has a local minimum. For a considerably large range of parameters, the minimum of C is reached at $\varphi_i \sim 10$, which corresponds to the maximum temperature increase during radial compression. Thus, in order to heat the plasma the most, we need to stay near this value, and vice versa to avoid it if we do not want extra heating.

IV. NUMERICAL EQUILIBRIUM

The numerical equilibrium solution for the compression function is worth some comment. The expression for radial compression function contains a pressure term in the denominator that came here from the pdV work term in the energy conservation equation. When the spinning parameter gets large, the pressure increases dramatically, as most of the particles hug the wall and very few particles are left in the center. As a result, it causes a problem of numerical resolution. We define our numerical solution on a grid, where the density is found as the total number of particles in a cell (the region between the two closest grid points). Apparently, for large φ, we have an extremely high density in the last several cells and nearly zero everywhere else. When we calculate the pressure, we need to take the density on the periphery, but we have only the mean density in the last cell, which is close, but not close enough, due to high numerical error caused by particles hugging the wall. As a consequence, the result for C can blow up if a certain accuracy is not reached.

There are three obvious ways of solving this problem: (i) use non-uniform grid, making more cells in the boundary zone and fewer in the center; (ii) include higher order derivatives in calculation of density on the wall; and (iii) increase the overall number of grid points for a better resolution. We tried all of these methods, and they all improved the accuracy; however, none of them and even their combination were stable for high enough Q, unless we increased the number of grid points so much that increased the computational time by several orders of magnitude.

The less obvious, but far superior way to solve this issue is to calculate the pressure as a derivative of the Helmholtz free energy F, using the thermodynamic relation $\partial F/\partial V = -p$. In the rotating frame, the Helmholtz free energy for particular species may be written as

$$F_{i,e} = -NT\ln\left(\frac{e\pi r_0^2 L}{N}\frac{mT}{2\pi\hbar^2}\int_0^1 2x dx \exp\left(\varphi_{e,i}x^2 \pm 2Q\Phi\right)\right) \tag{25}$$

and the total free energy is $F = F_i + F_e + W_E$. Taking the partial derivative of F with respect to r_0 (again, numerically) we obtain the desired pressure term. This method turned out being extremely stable and accurate; since the free energy has an integral form, it dramatically suppresses all numerical errors. We benchmarked this method with the exact solution for the non-charged case and with all three of the obvious methods (pushed to extreme accuracy).

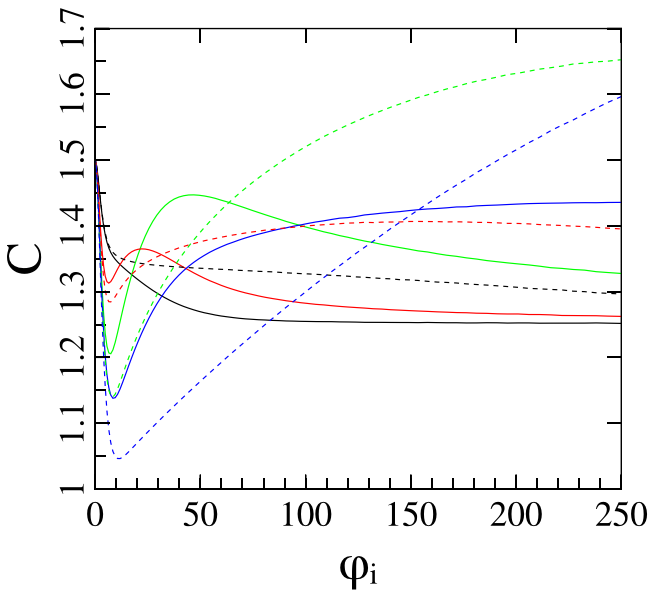

FIG. 5. Radial compression function for $c_v = 1.5$. Solid: $m_i/m_e = 10$; dashed: $m_i/m_e = 100$. Black: $Q = 0$; red: $Q = 4.5$; green: $Q = 40.5$, blue: $Q = 364.5$.

V. CONCLUSIONS AND DISCUSSION

The analysis presented here shows how the heat capacity and compressibility of rotating gases is altered when the gases are ionized. The key finding is that the radial electric field can indeed act to store energy, but the amount of energy that can be stored electrostatically, which is a function of the spinning rate and the mass ratio, is limited. For low spinning rate, and large mass ratio, the heat capacity is governed by the heavier species. For very high spinning rates, the heat capacity is governed by both species, but then the electrostatic energy is small. It is for intermediate spinning rates that the electrostatic energy plays an important, but not dominant, role in the heat capacity. At most, the increase in the heat capacity compared to the neutral spinning gas is on the order of the increase in the heat capacity of the spinning gas compared to the non spinning gas. This logic can be well illustrated in Fig. 6 that demonstrates how normalized electrostatic W_E/T energy depends on φ_i and Q. For both parameters, large enough W_E flattens out, therefore its derivatives, which determine the heat capacity contribution, are small. The sharpest gradients of W_E are at moderate values of φ_i and Q, where exactly the heat capacity difference is most noticeable.

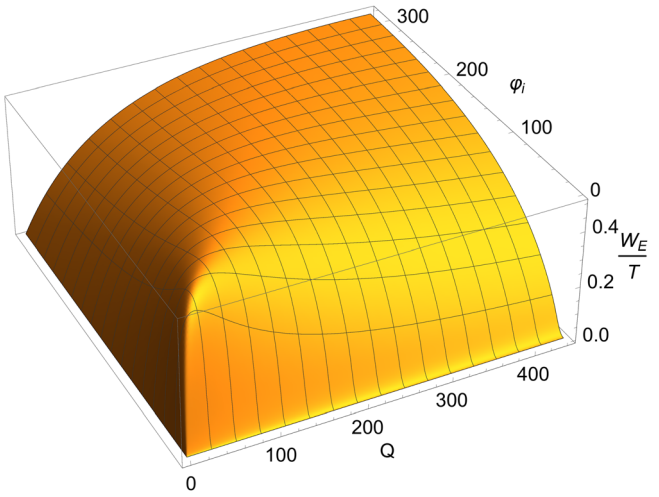

FIG. 6. Normalized electrostatic energy as a function of parameters Q and φ_i for $m_i/m_e = 10$.

While limited, this further increase in the heat capacity is still significant. It is hard to predict what applications can come from the further increase in heat capacity due to the ionization, however, in case of the increase in the heat capacity due to the spinning alone in neutral gas, an interesting application that emerged in the area of internal combustion engines run at a low temperature to avoid NOx emissions.[10] This made use of the fact that using the spinning gas as a working body for internal combustion engines increases the theoretical engine efficiency for the Otto cycle, an effect that is more pronounced at lower temperatures so that it may be worth the extra complexity in producing the spinning. It remains to be seen whether the increase in heat capacity of spinning plasma might be exploited in Z-machine compression, perhaps somewhat along suggestions for exploiting the energy contained in a turbulent motion[11] or coherent wave motion.[12]

The plasma heat capacity effect calculated here includes the energy in rotation as well as the self-consistent electrostatic energy. There are other types of turbulent or hydrodynamic motion that could also play a role of extra energy storage, or heat capacity, such as the turbulent kinetic energy that apparently appears under certain conditions in Z-pinch compression.[13,14] Compression of turbulence or vortices can amplify their energy that leads to increased heat capacity as well. However, compression should be done faster than the viscous dissipation time, besides, strictly speaking, the system is not in equilibrium, and the heat capacity is no longer defined as a thermodynamical state function. These extra stored energy can suddenly dissipate to thermal energy[11,15] that open new possibilities to energy transformation and even fusion approach.

Several generalizations of this new physical effect can be anticipated. An obvious generalization is to the case of partially ionized gas or to a mixture of several multi-ionized species of different masses. A second obvious generalization is to include an axial magnetic field; the simplest generalization is where the rotation and thermal speeds are small so that only a constant magnetic field needs to be considered, with the plasma generated magnetic fields being negligible. The further straightforward generalization is to include both the plasma diamagnetism as well as the self-generated fields through the spinning of charge.

In all of the above, we assume that, under compression, the plasma remains near thermodynamic equilibrium, so that an equation of state is obtainable just like for the adiabatic compression of ideal gases. However, even under very slow compression, there are interesting dynamical effects to consider. First, particularly in the presence of a magnetic field, there can be instabilities with growth rates possibly on the time scale of the compression (see, e.g., Refs. 16–18). Second, even in the absence of the magnetic field, and even under slow compression, but fast enough compared to the heat diffusion time, we can anticipate a generalized *piezothermal effect*. The piezothermal effect for neutral gas results in a temperature gradient transverse to the direction of compression, but parallel to the gradient of either an external or internal potential.[19] In case of spinning plasma, there are both centrifugal and electrostatic forces in the radial direction, so the conditions for the piezothermal effect are met for compression in the axial direction. However, since these forces are strongly coupled, it remains to be calculated, quite, how the piezothermal effect in spinning plasma will quantitatively express itself.

ACKNOWLEDGMENTS

This work was supported by DTRA, DOE Contract No. DE-AC02-09CH11466, and by NNSA SSAA Grant No. DE-NA0002948.

[1]M. J. Thompson, *An Introduction to Astrophysical Fluid Dynamics* (Imperial College Press, London, 2006), Chap. 9.
[2]D. J. Ampleford, S. V. Lebedev, A. Ciardi, S. N. Bland, S. C. Bott, G. N. Hall, N. Naz, C. A. Jennings, M. Sherlock, J. P. Chittenden, J. B. A. Palmer, A. Frank, and E. Blackman, Phys. Rev. Lett. **100**, 035001 (2008).
[3]M. J. Bennett, S. V. Lebedev, G. N. Hall, L. Suttle, G. Burdiak, F. Suzuki-Vidal, J. Hare, G. Swadling, S. Patankar, M. Bocchi, J. P. Chittenden, R. Smith, A. Frank, E. Blackman, R. P. Drake, and A. Ciardi, High Energy Density Phys. **17**, 63–67 (2015).
[4]M. Bocchi, B. Ummels, J. P. Chittenden, S. V. Lebedev, A. Frank, and E. G. Blackman, Astrophys. J. **767**(1), 84 (2013).
[5]M. Bocchi, J. P. Chittenden, S. V. Lebedev, G. N. Hall, M. Bennett, A. Frank, and E. G. Blackman, High Energy Density Phys. **9**, 108–111 (2013).
[6]D. D. Ryutov, Astrophys. Space Sci. **336**, 21–26 (2011).
[7]V. I. Geyko and N. J. Fisch, Phys. Rev. Lett. **110**, 150604 (2013).
[8]L. D. Landau and E. M. Lifschitz, *Statistical Physics I* (Pergamon Press, Oxford, 1968), Chap. 2.
[9]P. C. Clemmow and J. P. Dougherty, *Electrodynamics of Particles and Plasmas* (Addison-Wesley, Redwood City, CA, 1969).
[10]V. I. Geyko and N. J. Fisch, Phys. Rev. E **90**, 022139 (2014).
[11]S. Davidovits and N. J. Fisch, Phys. Rev. Lett. **116**, 105004 (2016).
[12]P. F. Schmit, I. Y. Dodin, J. Rocks, and N. J. Fisch, Phys. Rev. Lett. **110**, 055001 (2013).
[13]E. Kroupp, D. Osin, A. Starobinets, V. Fisher, V. Bernshtam, L. Weingarten, Y. Maron, I. Uschmann, E. Förster, A. Fisher, M. E. Cuneo, C. Deeney, and J. L. Giuliani, Phys. Rev. Lett. **107**, 105001 (2011).
[14]Y. Maron, A. Starobinets, V. I. Fisher, E. Kroupp, D. Osin, A. Fisher, C. Deeney, C. A. Coverdale, P. D. Lepell, E. P. Yu, C. Jennings, M. E. Cuneo, M. C. Herrmann, J. L. Porter, T. A. Mehlhorn, and J. P. Apruzese, Phys. Rev. Lett. **111**, 035001 (2013).
[15]S. Davidovits and N. J. Fisch, Phys. Rev. E **94**, 053206 (2016).
[16]Z. Wang, J. Si, W. Liu, and H. Li, Phys. Plasmas **15**, 102109 (2008).
[17]G. Montani, R. Benini, N. Carlevaro, and A. Franco, MNRAS **436**, 327 (2013).
[18]S. Chandrasekhar, Proc. Natl. Acad. Sci. U.S.A. **46**(2), 253–257 (1960).
[19]V. I. Geyko and N. J. Fisch, Phys. Rev. E **94**, 042113 (2016).